

Gangotri mission concept on the glacial key to the Amazonian climate of Mars

Suniti Karunatillake¹, Juan Lorenzo¹, Lujendra Ojha², Scott M. Perl³, Katherine Mesick⁴, Paul Niles⁵ and the Gangotri team (<https://doi.org/10.3847/25c2feb.a3d8d8e9>)
¹Geology & Geophysics, Louisiana State University (sunitiw@lsu.edu); ²Rutgers University; ³NASA-JPL; ⁴LANL; ⁵NASA-JSC

NASA Tech Showcase, 2023 Abstract
<https://nasa-techshowcase.seti.org/abstracts/>

The wealth of geologic information bound in martian ice (Figs. 1, 2), including climate cycles, potential biomarkers, atmospheric particulates, and sources of H₂O that may drive alteration within the critical zone (CZ: zone of interaction between the atmosphere and the porous upper crust) has long been recognized (Figs. 6, 8). Much progress has been made in the last decade, in interpreting polar ice sheet [Bapst et al., 2019] and midlatitudinal ice [e.g., Dundas et al., 2018; Harish et al., 2020; Piqueux et al., 2019] processes.

Despite recent advances, outstanding questions remain at the forefront of exploration [cf., Bramson et al., 2021]. Martian midlatitudes provide a notable opportunity to explore these in the evolution of ice beyond the poles (Figs. 1, 2), as emphasized in the National Academies of Sciences 2023-2032 decadal survey's general Mars Life Explorer outline [2022]. Including the examples in Figs. 4 and 5, such glaciers are ablating as evident from scarps, boulder fields, and pits [Dundas et al., 2018]. Accordingly, our mission concept—aptly eponymous with the large and fast-receding Himalayan glacier, Gangotri—would investigate the geologic origins of midlatitudinal martian glaciers. Gangotri would help to characterize Amazonian climate evolution via Honeybee Robotics' hybrid thermo-mechanical drill [Mellerowicz et al., 2022] for deep and possibly multiple englacial sampling, including for in situ resource use (Fig. 7). Gangotri would use regolith compositional measurements to analyze ice-regolith interaction, and stable isotope measurements to characterize fundamental exchange processes (Fig. 8) of major ice reservoirs (Fig. 3). Meanwhile, geophysical observations would cross-calibrate composition, with sensitivity to the presence of brines or meltwater. Example platform and payload are shown in Figs. 9a-i, linked to the science traceability matrix (Table STM-A, B), and spacecraft architecture (Table SA).

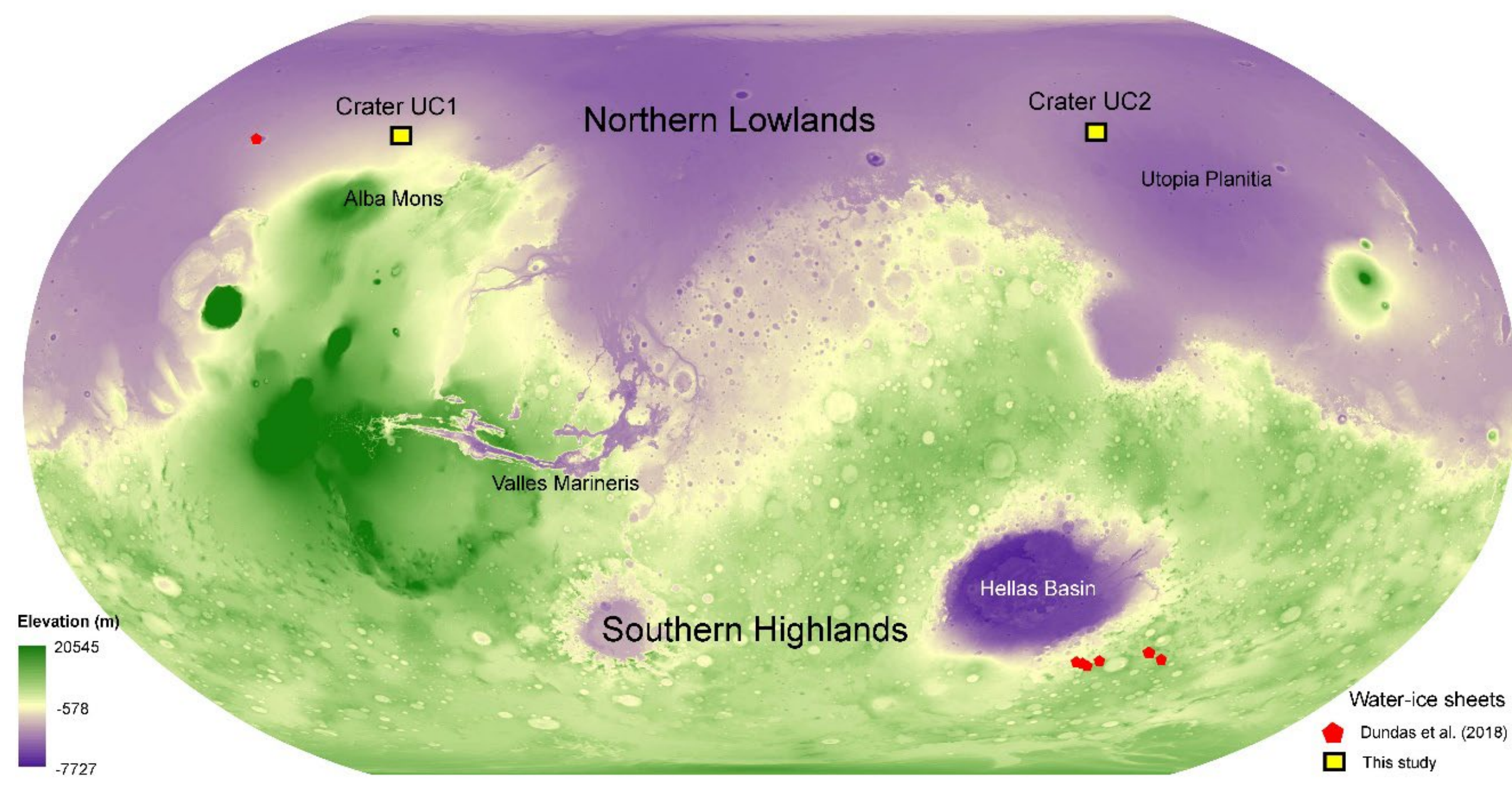


Figure 1. Sites of martian ground ice determined from satellite infrared spectroscopy (MRO-CRISM) and optical imagery (MRO-HiRISE). As in Figs. 4 and 5, ground ice occurs at hundreds of meter (intra-crater: UC1, UC2) and up to tens of km (red icons) lateral scales. Some ice sheets likely **hundreds of meters thick**. From the work by Harish et al. [2020].

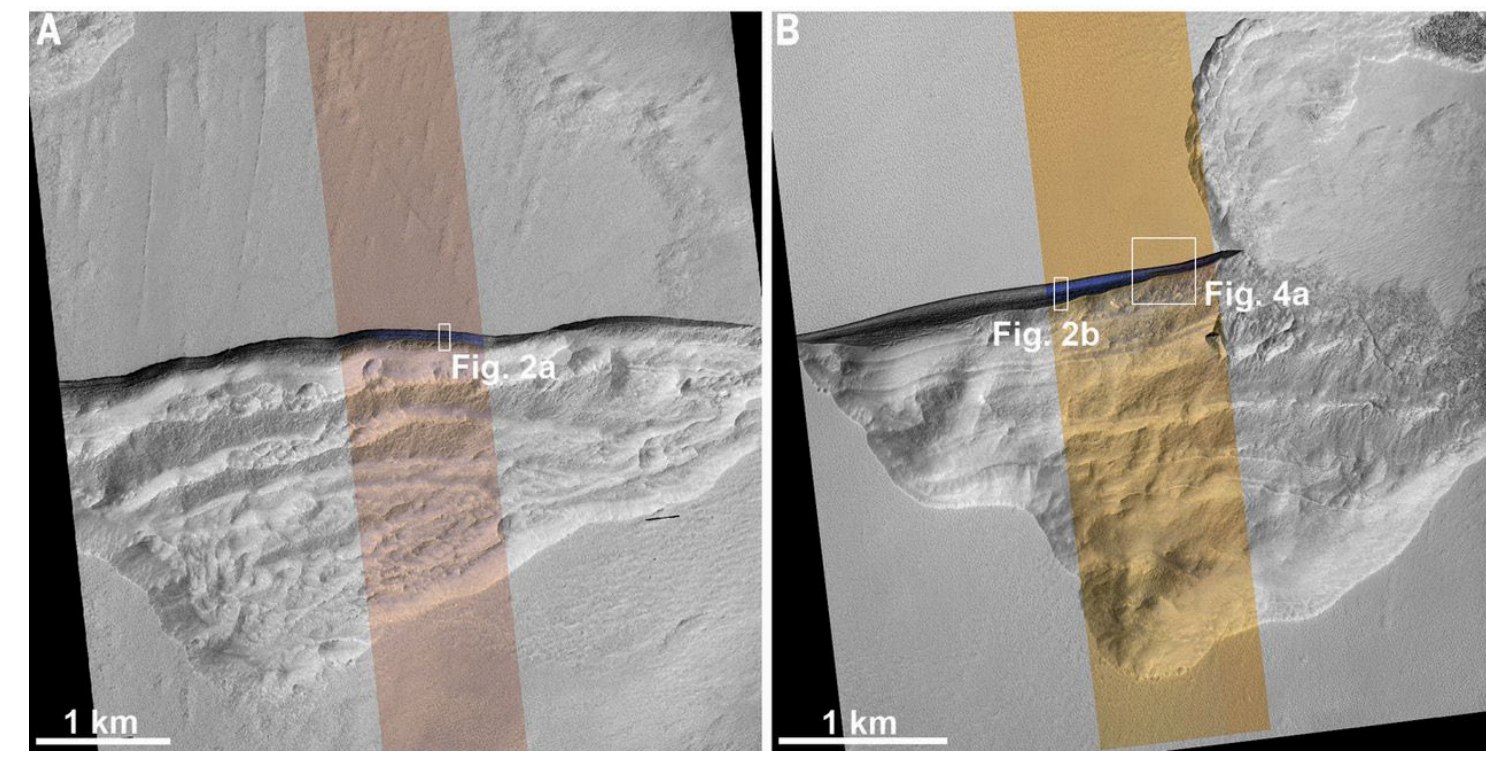


Figure 4. Example of southern mid-latitudinal ice sheet with collapse scarps and pitting (Geographic and geochemical context in Figures 1 and 2, respectively). By Dundas et al. [2018].

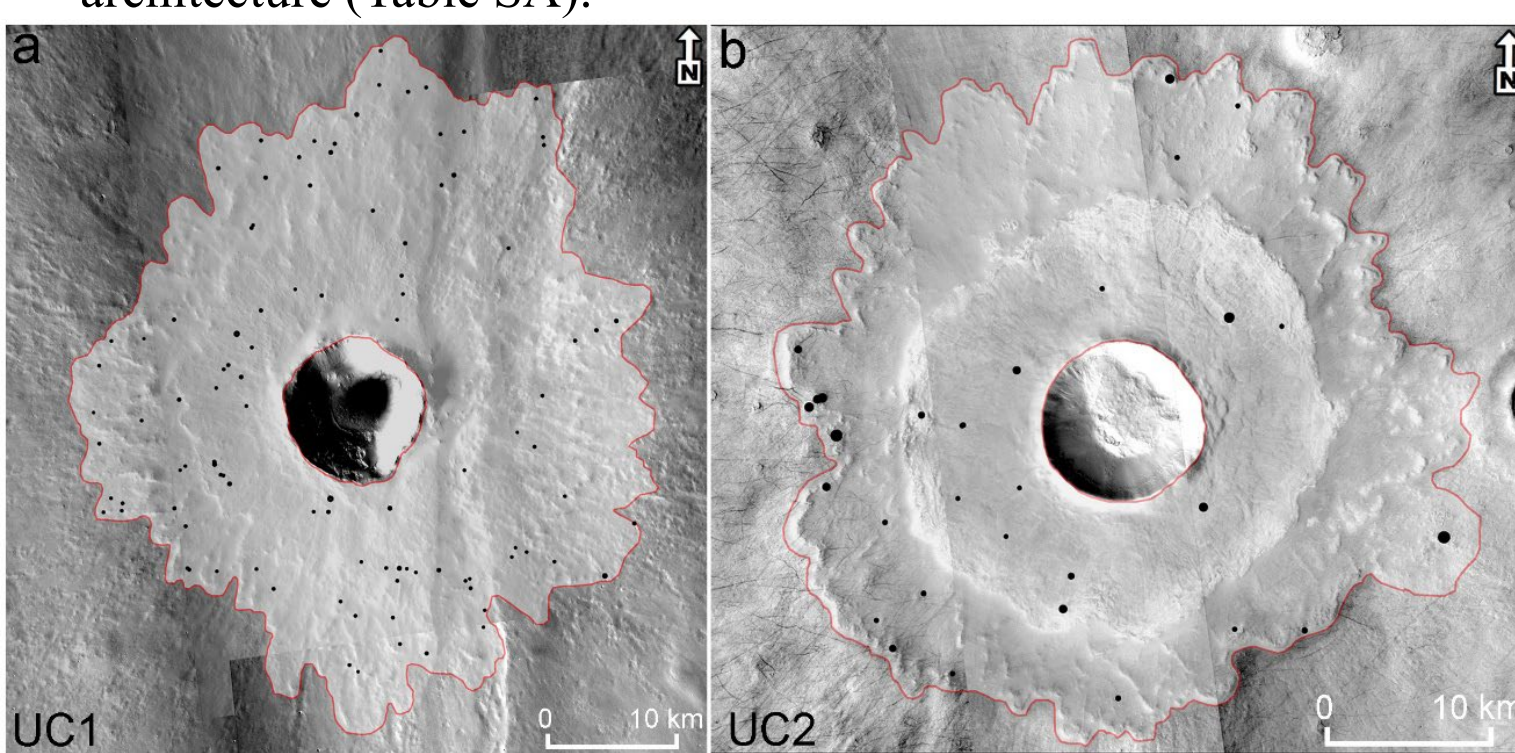


Figure 5a. Two mid-latitudinal craters in the northern hemisphere showing fluidized ejecta morphology and bearing ice within. Figures 1 and 2 show geographic and geochemical context. [Harish et al., 2020]

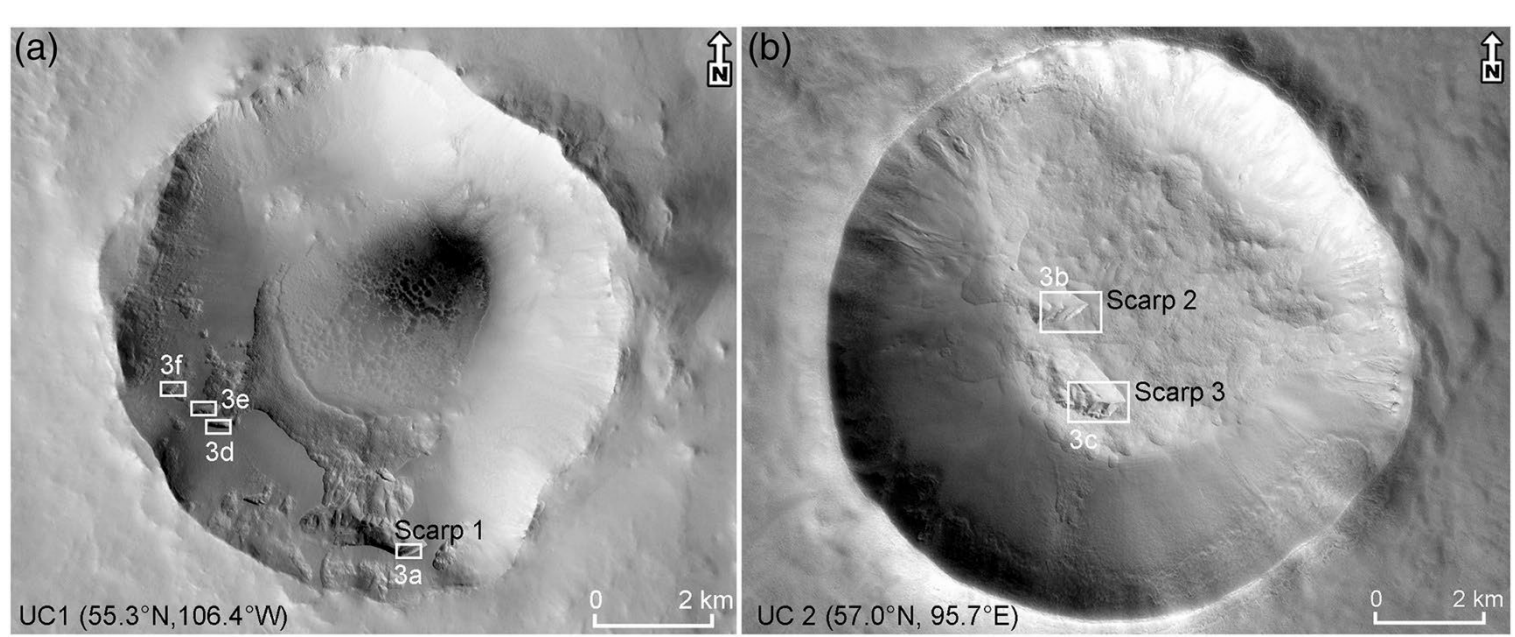


Figure 5b. Magnified view of the floor ground ice units for the crater shown in Figure 5a. [Harish et al., 2020]

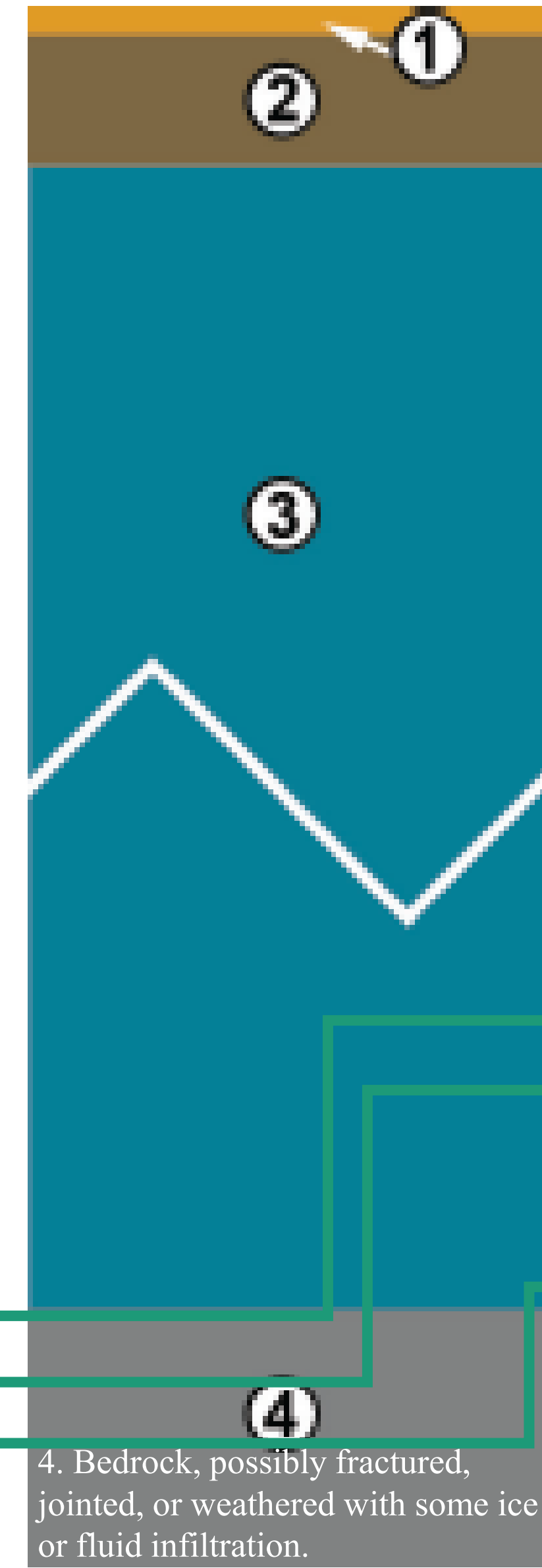
Table STM-A. Science Traceability Matrix A (STM-A) for the GANGOTRI Mission Concept. For legibility and conceptual flow, STM is bifurcated, one relating mission goals and aims to NASA goals (Table STM-A), and the other associating mission aims with physical parameters, observables, and performance requirements (Table STM-B). For brevity, we only excerpt relevant text with ellipsis (...) of the NASA Visions and Voyages 2013–2022 decadal survey (DS) [NRC, 2011], mid-term review (MTR) [NAS, 2018] and NASA's science plan (SP) [2014]. The Committee on Astrobiology and Planetary Sciences (CAPS) report [NAS, 2017] identifies Mars as a key target for each DS goal excerpted.

Examples of NASA Goals	GANGOTRI Science & Human Exploration Goals	GANGOTRI Objectives (Aims)
DS: How do the climate, and especially the water cycle, vary with orbital and obliquity variations? ... more detailed examination of ... layered sedimentary rocks for the record of climate ... to improve the understanding of volatile budgets and cycles.	SG. Understanding climate-driven processes of mid-latitudinal glaciers as a key H ₂ O reservoir within Mars's critical zone.	SG1. Test the latest H ₂ O reservoir exchange model for Mars using DH isotopic signatures. SG2. Resolve a paradoxical divergence between theoretical and observed atmospheric DH variance for Mars. SG3. Determine the extent to which englacial siliciclastics and sulfate-rich aerosols undergoing low-pH alteration may yield Martian sulfate sedimentary strata.
DS: ... understanding of the astrobiological potential of the observable water-ice deposits.	SB. Determining the habitability and biomarker preservation potential of young Martian glacioclasts.	SB1. Determine the extent to which ancient organics and microorganisms can be deposited, unmixed, and preserved in young glaciers. SB2. Determine whether any presence of organics and microorganisms was driven by aeolian-deposited glacial dust.
DS: To reduce the cost and risk for future human exploration, robotic ... missions ... to secure information concerning potential resources. ... investigating the distribution of shallow excess ice will quantify an important resource to provide astronauts with water and oxygen. ...	HE. Establish a ground-truth reference volume for H ₂ O ice as a possible ISR. HE2. Identify which glacial H ₂ O extraction and purification methods would be optimal for ISR use. HE3. Determine forward and backward biological contamination thresholds before using readily accessible Martian ice as an ISR.	HE1. Establish a ground-truth reference volume for H ₂ O ice as a possible ISR. HE2. Identify which glacial H ₂ O extraction and purification methods would be optimal for ISR use. HE3. Determine forward and backward biological contamination thresholds before using readily accessible Martian ice as an ISR.

Table SA. Spacecraft architecture (SA) for the GANGOTRI mission concept

Component	Heritage or TRL	Details	Expected Mass (kg)
EDL Platform	M2020	EDL Platform and landing system based on the sky crane system adapted for the weight and momentum of the GANGOTRI rover.	2400 [NASA]
Rover	M2020	Rover chassis as the base design. Key enhancements include wheel design for enhanced excavating ability, Radioisotope Power System (RPS) optimization for the drill and rover, and acoustic seismometer integration into wheels.	900 [NASA]
Thermo-mechanical Drill	RefWat	Thermal source options, cooled tubing drill configuration, sample preparation, and sample delivery to the deck are key areas for development. Likewise, science payload consisting of dust logger, fluorometer, and microscope are to be incorporated.	75
MHS	M2020	MHS imaging systems will be modified for mapping.	1.81 [Agie, 2019]

Figure 3. Conceptual schematic of glacial profile for mission sampling



1. Dry soil, including tens of micron size dust grains, forming a mantling unit cm – m thick over ice sheets
2. Underlying permafrost equivalent ice rich soil unit(s) of meter depth scales.
3. Ice layers, possibly containing unconformities, bedding, laminations and massive units. Primary archive of climatologic and geologic (e.g., globally dispersed volcanic ash columns) events. May reach 0.1 – 0.2 km depths in places (Fig. 4).
4. Bedrock, possibly fractured, jointed, or weathered with some ice or fluid infiltration.

Table STM-B

Required physical parameters	Required observables	Platform and mission performance requirements
SO1 SR1. Engliacial hydrogen isotopic abundance	SO1. Mass spectrometry of DH molar ratios	SP1. SAM specifications with 6D resolution (2SD) of ±100‰
SO2 SR2.1 Engliacial hydrogen isotopic variations	SO2.1 Same as SO1	SP2.1 Same as SP1
SO2 SR2.2 Climate & weather governing glacial instability	SO2.2 Local temperature, pressure, wind velocity, and humidity over 1 Mars year	SP2.2 MEDA specifications, corrected for the spacecraft's thermal effects.
SO2 SR2.3 Overnight energy exchange at glacial sites	SO2.3 Thermal characterization with infrared spectroscopy	SP2.3 MiniTES specifications
SO3 SR3.1 Extremeness, composition, and layering of englacial siliciclastics, salts, and trapped gases, including dust-shed layers.	SO3.1.1 Relative englacial abundances of phyllosilicates, percolates, sulfates, and other mineralogical and amorphous components.	SP3.1.1 SAM evolved gas chromatography and mass spectrometry operating up to 800 °C with 70 μg/kg sensitivity to evolved volatiles.
SO3 SR3.2 Complementary isotopic measurements of H, C, O, S, and Cl	SO3.1.2 Complementary isotopic measurements of H, C, O, S, and Cl	SP3.1.2 Same as SP3.1.1
SO3 SR3.3 Optical scattering by englacial dust	SO3.1.3 Optical scattering by englacial dust	SP3.1.3 Dust logger with 405 nm laser to illuminate surrounding glacial ice in a horizontal fan (90° wide) at 1–2 mm vertical resolution in backscatter mode.
SR2.2 Contextual surface geochemistry and mineralogy across overlying regolith and ground ice boundary	SO2.2.1 Bulk regolith concentration of major silicate forming elements (Fe, Si, Al, Ca, Mg), mobile elements significant for brine activity (Cl, S, H), and large ion lithophiles significant for distinguishing aqueous versus igneous processes (K, Th).	SP2.2.1 NGRS with better than 15% precision for targeted elements.
SO2.2.2 Infrared spectroscopy of vertical minerals	SO2.2.2 Infrared spectroscopy of vertical minerals	SP2.2.2 MiniTES infrared spectral resolution specification
SO2.2.3 Compositional and physical stratification across the regolith-ice boundary layer	SO2.2.3 Compositional and physical stratification across the regolith-ice boundary layer	SP2.2.3 Piezo-ceramic acoustic seismometer with 1 kHz bandwidth of finer than 10 m vertical resolution, and SP2.2.4
SB1 Type abundance of aromatic organic molecules and microbial cell components	SB1.1 Evolved gas chromatograph mass spectrometry	SB1.1.1 SAM system using retention times on the gas chromatograph and full separation of isobaric interferences.
SB2 Physical association between organic molecules, microbial cell components, and siliciclastics	SB2.1 UV fluorometric detection of organics and microbial cells	SB2.1.1 UV fluorometer with up to 4 excitation wavelengths, 16 emission channels, and micro-resolution sensitive to 50–100 cells/mL.
SB3 UV microscopic imaging of organics, microbial cell components, and granular material	SB3.1 UV microscopic imaging of organics, microbial cell components, and granular material	SB3.1.1 Sample staining sub-micro resolution UV microscope with 10, 1, and 0.1 μM scales for mud slurry
HE1 Depth, lateral extent, and concentration of H ₂ O ice	HE1.1 Geologic mapping with optical imagery	HE1.1.1 MHS imaging at 10–30 μm/pixel resolutions for km scale aerial surveying
HE2 Chemical (e.g., sulfates) and physical (e.g., siliciclastics) constituent abundance in ice	HE2.1 Same as SO3.1.3, SO3.2.1, & SO3.2.3	HE2.1.1 Same as SP3.1.3, SP3.2.1, SP3.2.3
HE3 Microbial or biogenic material in ice	HE3.1 Same as SB1.1, SB2.1, SB3.1	HE3.1.1 Same as SB1.1, SB1.2, SB1.3.1, SB1.3.2
All All except SR2.2, SR2.3, SR3.2	All except SO2.2, SO2.3, SO3.2.1, SO3.2.2, SO3.2.3 and HE1.1	Hybrid thermo-mechanical drill penetrating 10–30 m depths. Sample preparation-delivery system from borehole to rover deck.

Fig. 9 Example rover concept and payload



Fig. 9b. Mars Environment Dynamic Analyzer (MEDA) to characterize glacial micro-climate. [Rodríguez-Manfredi, 2021]

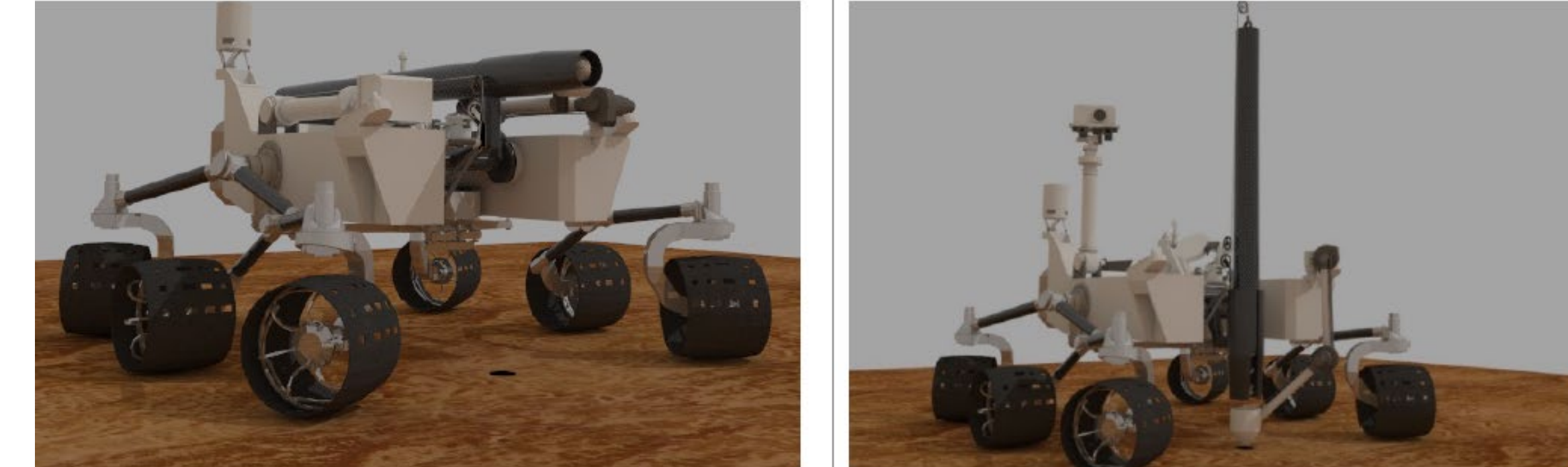


Fig. 9c. Mobile to stationary rover-based platform to sample the glacial column at an optimal site for the science traceability matrix (Tables STM-A, B). Mobility will also enhance recoverability from unforeseeable drill obstructions by relocating to alternative sites.

Fig. 9d. Sample Analysis at Mars (SAM) module optimized for isotopic geochemistry of key elements (e.g., H, S). Mounted on-deck to analyze slurry (ice, fluid, silicate, salt mix) extracted during drilling. [cf., Franz et al., 2014, 2017; Mahaffy et al., 2012]

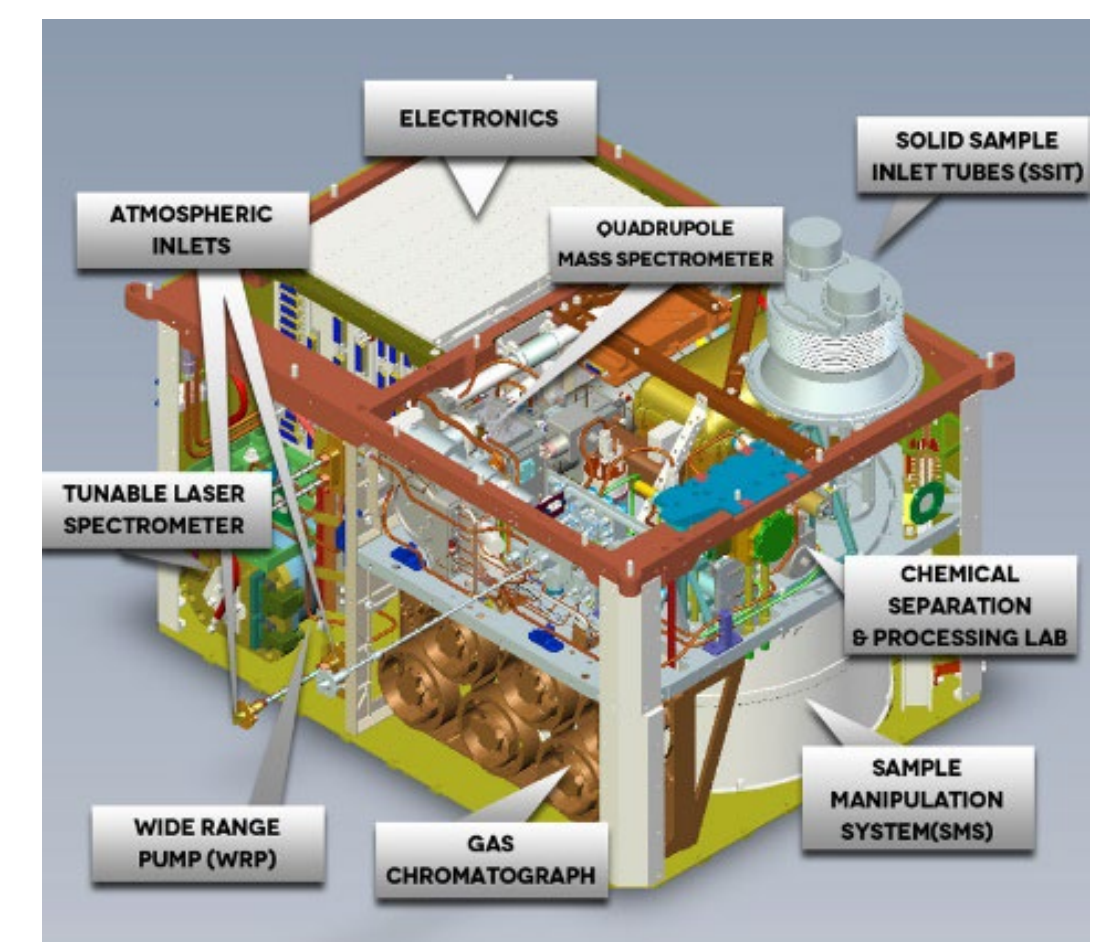


Fig. 9e. Wheel-mounted low-resolution seismometer at high (acoustic) frequency for soil-ice boundary layer insight at meter depths scales. [Lorenzo et al., 2022]

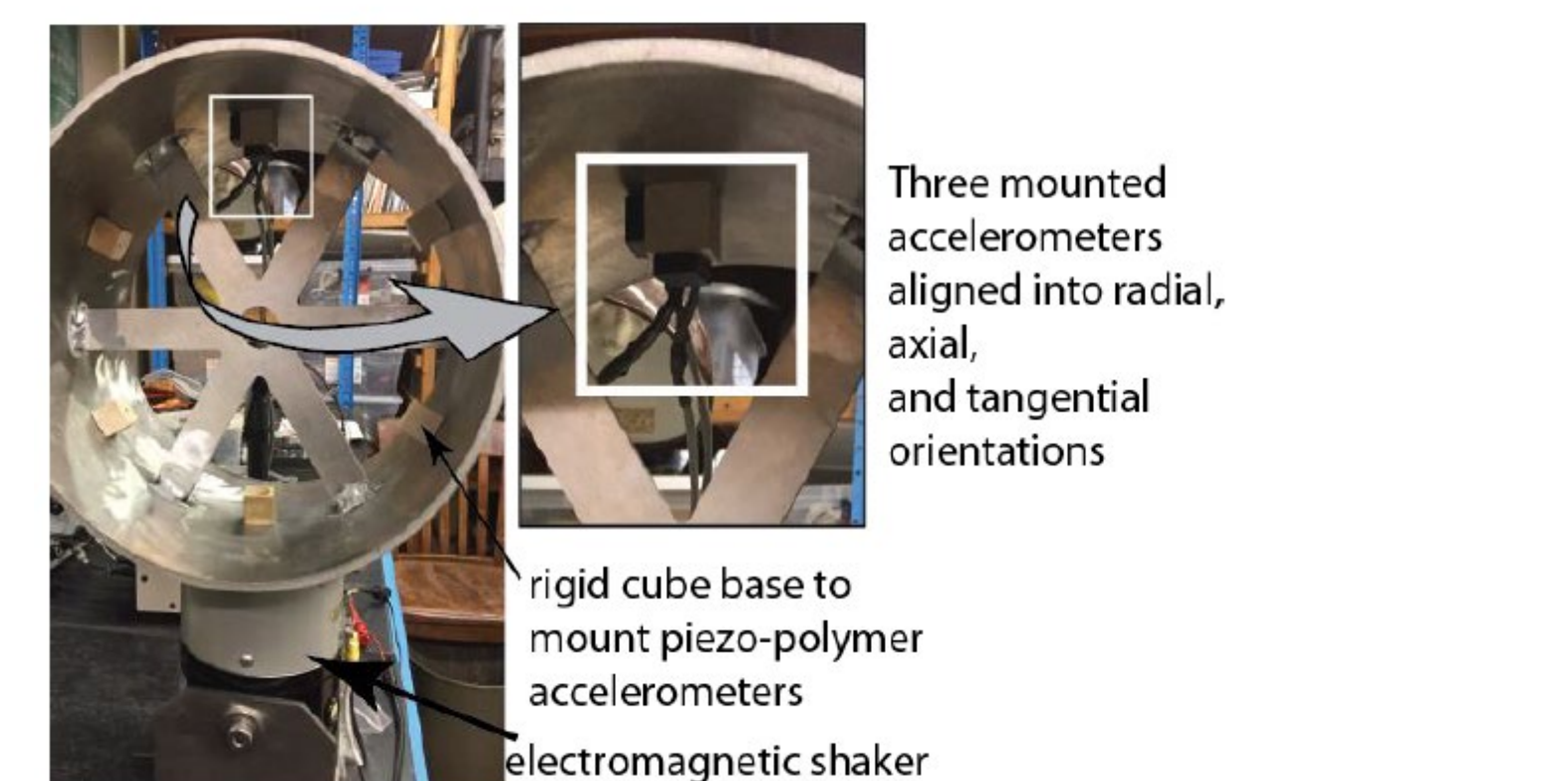


Fig. 9f. Deck-mounted neutron-gamma spectrometer (NGRS) for geochemical characterization. Tables STM-A, B show key elements for geology and habitability characterizations. [Mesick et al., 2018]

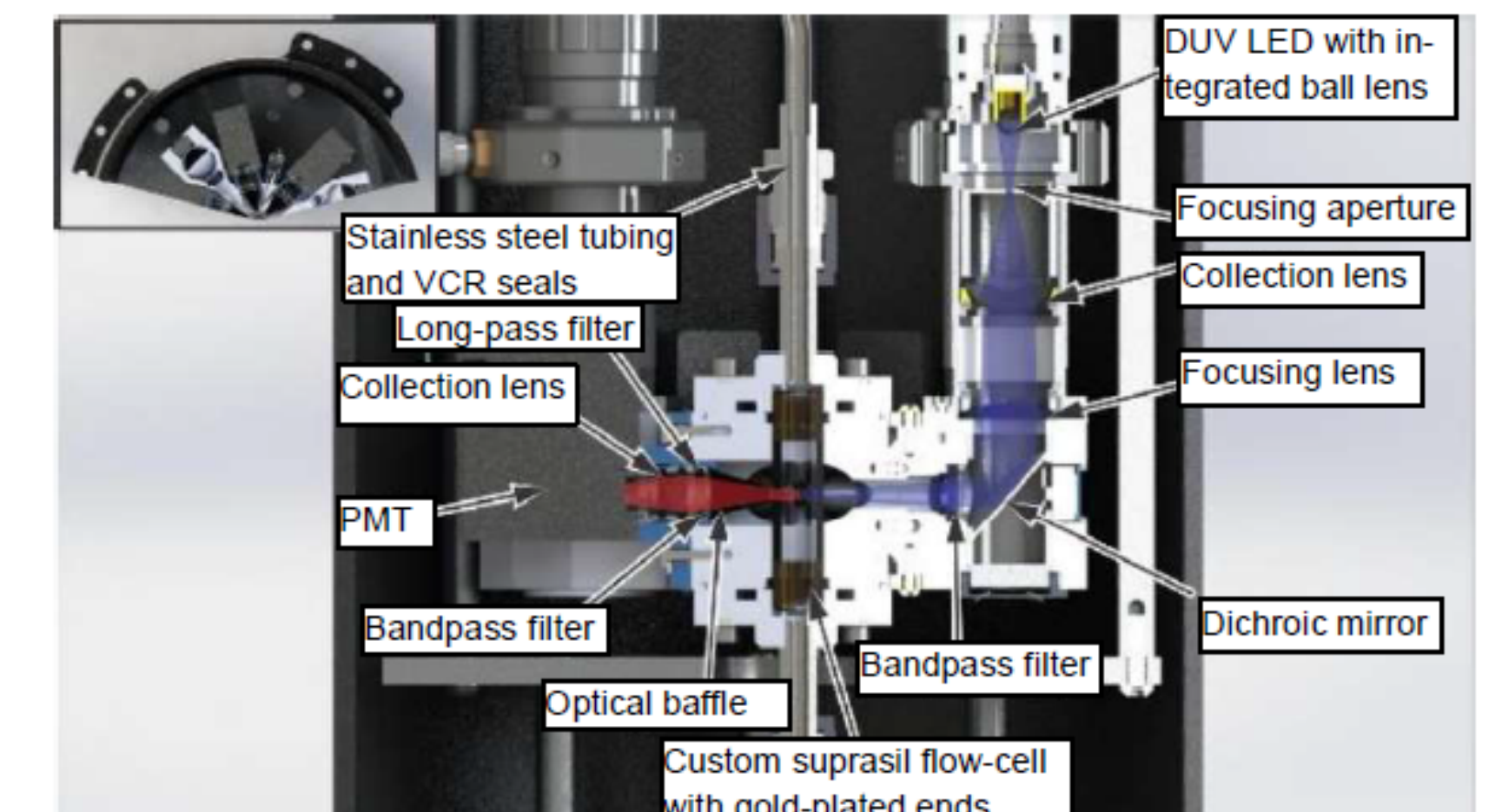
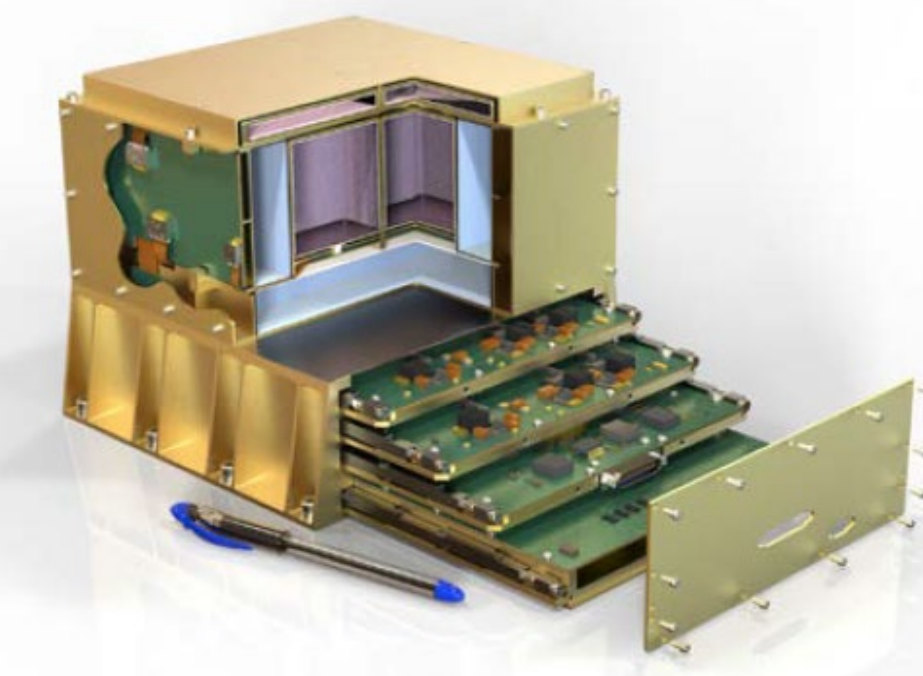


Fig. 9g. Thermo-mechanical drill for tens of meter englacial sampling capability. Honeybee Robotics RedWater design shown as example. Ducts to extract sample slurry for analyses with deck-instruments, tether and emergency-jettison systems, as well as embedding analytical payload are needed. [Mellerowicz et al., 2022]

Fig. 9i. Drill-embedded dust logger for insight into climatic cyclicity and episodic deposition from silicate sediment in the glacial column. Example spectra from Antarctic sites. [Bramall et al., 2005, 2007]

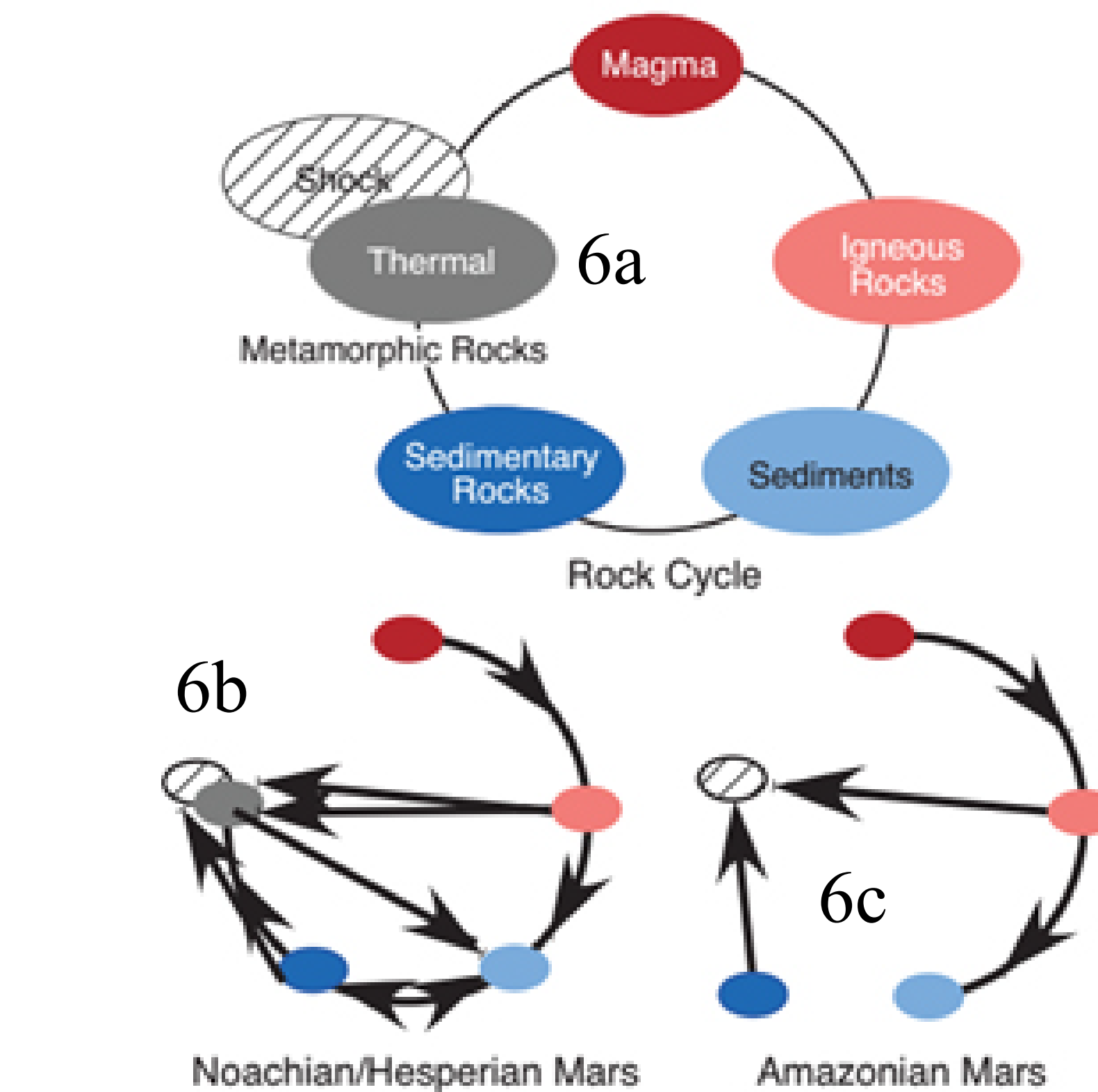
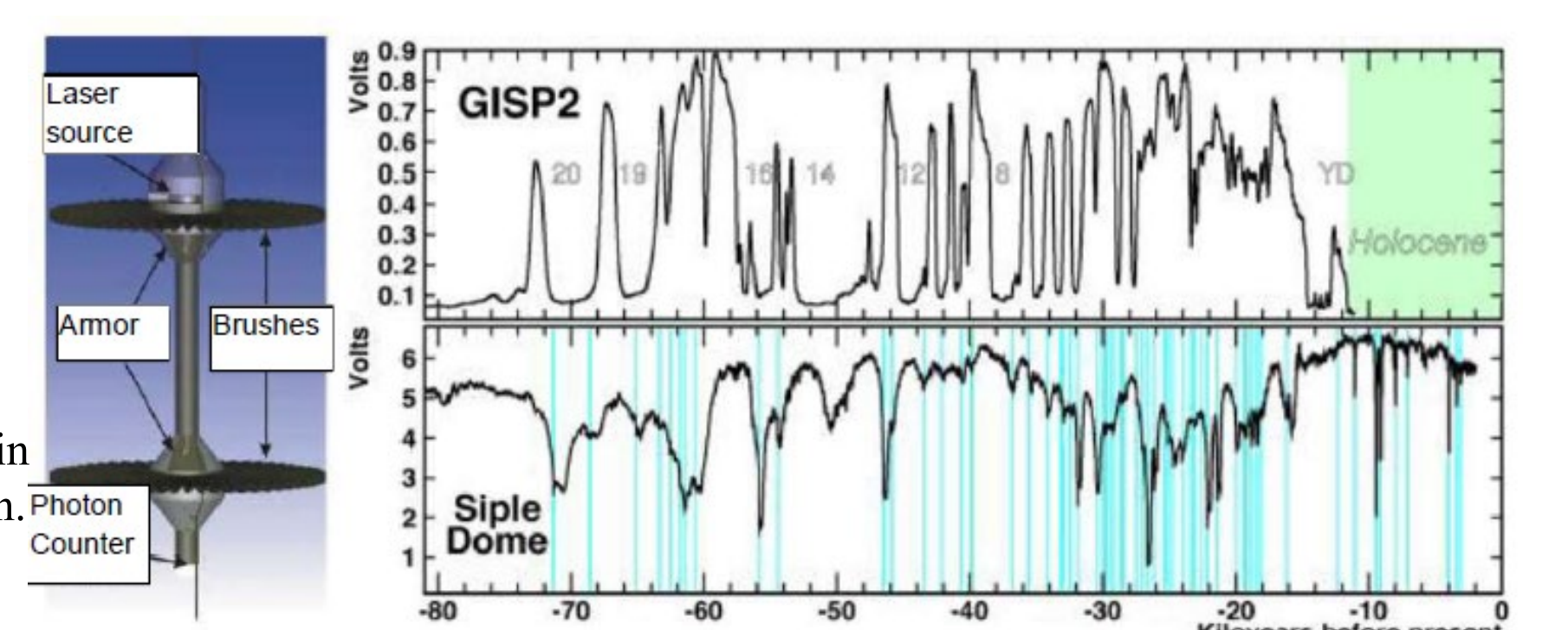


Figure 6. Unknowns in the martian rock cycle to be investigated with a mid-lat glacial mission. A: Earth's rock cycle, color-coded for reference. B: Ancient Mars, with the recycling of sedimentary rocks into magma poorly known. C: Additional gaps in modern Mars, particularly on sediment diagenesis or lithification. Weathering of englacial sediment by brines in ice, scavenging SO₂-phases, may be a possible pathway. [McSween, 2015]

Figure 7. Artist's rendering of in situ resource use for sustaining human habitats. Martian ice units could prove invaluable, but require assessment of forward-backward biologic contamination, construction of extraction facilities at supra- or peri-glacial landscapes, and mitigated toxicity risks of ice-entrained phases, such as sulfates, or particulates, such as volcanic ash.

Figure 8. H₂O exchange reservoirs in the martian critical zone during celestial mechanics of the last few Ma. The layering in mid-latitudinal ice sheets, as targeted by GANGOTRI, would archive isotopic signatures of H₂O exchange with high-altitudes (e.g., Olympus Mons) and the polar zones. Current model for NPLD can be refined and cross-calibrated with celestial mechanics models by sampling the mid-latitudinal glacial strata. [Vos et al., 2019]

ACKNOWLEDGMENTS
 Louisiana State University Faculty Research Grant Program Big Idea, Phase 3, Proposal 3649.
 Ernest & Alice Neal Professorship in Geology & Geophysics
BIBLIOGRAPHY
 Balaram (2021) [10.1007/s11214-021-00815-w](https://doi.org/10.1007/s11214-021-00815-w); Bapst et al. (2019) [10.1029/2018JE005786](https://doi.org/10.1029/2018JE005786); Bramall (2005) [10.1029/2005GL024236](https://doi.org/10.1029/2005GL024236); Bramall (2007) [10.1029/2006GL024236](https://doi.org/10.1029/2006GL024236); Dundas (2018) [10.1126/SCIENCE.AAO1619](https://doi.org/10.1126/SCIENCE.AAO1619); Franz (2014) [10.1016/j.jps.2014.03.005](https://doi.org/10.1016/j.jps.2014.03.005); Franz (2017) [10.1038/ngeo3002](https://doi.org/10.1038/ngeo3002); Harish (2020) [10.1029/2020GL089057](https://doi.org/10.1029/2020GL089057); Lorenzo (2022) [10.1100/tecl11006811](https://doi.org/10.1100/tecl11006811); McSween (2015) [10.2138/am-2015-5257](https://doi.org/10.2138/am-2015-5257); Mellerowicz (2022) [10.1089/SPACE.2021.00577](https://doi.org/10.1089/SPACE.2021.00577); Mahaffy (2012) [10.1007/s11214-012-9879-z](https://doi.org/10.1007/s11214-012-9879-z); Mesick (2018) [10.1109/NSSMIC.2018.8824376](https://doi.org/10.1109/NSSMIC.2018.8824376); Niles (2009) [10.1038/ngeo438](https://doi.org/10.1038/ngeo438); Piqueux (2019) [10.1029/2019GL083947](https://doi.org/10.1029/2019GL083947); National Research Council (2011) [10.17226/13117](https://doi.org/10.17226/13117); National Academies of Sciences (2017) [10.17226/24843](https://doi.org/10.17226/24843); NAS (2018) [10.17226/25186](https://doi.org/10.17226/25186); NAS (2022) [10.17226/26522](https://doi.org/10.17226/26522); SP 2014 <https://www.nas.nasa.gov/about-us/science-strategy/>; Rodríguez-Manfredi (2021) [10.1007/s11214-021-00816-9](https://doi.org/10.1007/s11214-021-00816-9); Vos (2019) [10.1016/j.jps.2019.01.018](https://doi.org/10.1016/j.jps.2019.01.018)